Geochemistry Geophysics Geosystems G3
AN ELECTRONIC JOURNAL OF THE EARTH SCIENCES
Published by AGU and the Geochemical Society

Article
Volume 6, Number 11
4 November 2005
Q11001, doi:10.1029/2005GC001013
ISSN: 1525-2027

Models of hydrothermal circulation within 106 Ma seafloor: Constraints on the vigor of fluid circulation and crustal properties, below the Madeira Abyssal Plain

A. T. Fisher

Earth Sciences Department, University of California, 1156 High Street, Santa Cruz, California 95064, USA (afisher@es.ucsc.edu)

Institute for Geophysics and Planetary Physics, University of California, Santa Cruz, California 95064, USA

R. P. Von Herzen

Department of Geology and Geophysics, Woods Hole Oceanographic Institution, Woods Hole, Massachusetts 02543, USA

Institute for Geophysics and Planetary Physics, University of California, Santa Cruz, California 95064, USA

[1] Heat flow measurements colocated with seismic data across 106 Ma seafloor of the Madeira Abyssal Plain (MAP) reveal variations in seafloor heat flow of ±10–20% that are positively correlated with basement relief buried below thick sediments. Conductive finite element models of sediments and upper basement using reasonable thermal properties are capable of generating the observed positive correlation between basement relief and seafloor heat flow, but with variability of just ±4–8%. Conductive simulations using a high Nusselt number (*Nu*) proxy for vigorous local convection suggest that $Nu = 2–10$ within the upper 600–100 m of basement, respectively, is sufficient to achieve a reasonable match to observations. These *Nu* values are much lower than those inferred on younger ridge flanks where greater thermal homogeneity is achieved in upper basement. Fully coupled simulations suggest that permeability below the MAP is on the order of 10^{-12}–10^{-10} m^2 within the upper 300–600 m of basement. This permeability range is broadly consistent with values determined by single-hole experiments and from modeling studies at other (mostly younger) sites. We infer that the reduction in basement permeability with age that is thought to occur within younger seafloor may slow considerably within older seafloor, helping hydrothermal convection to continue as plates age.

Components: 10,107 words, 8 figures.

Keywords: crustal evolution; hydrothermal processes; numerical modeling.

Index Terms: 3021 Marine Geology and Geophysics: Marine hydrogeology; 3017 Marine Geology and Geophysics: Hydrothermal systems (0450, 1034, 3616, 4832, 8135, 8424).

Received 10 May 2005; **Revised** 15 August 2005; **Accepted** 19 September 2005; **Published** 4 November 2005.

Fisher, A. T., and R. P. Von Herzen (2005), Models of hydrothermal circulation within 106 Ma seafloor: Constraints on the vigor of fluid circulation and crustal properties, below the Madeira Abyssal Plain, *Geochem. Geophys. Geosyst.*, *6*, Q11001, doi:10.1029/2005GC001013.

1. Introduction

[2] Seafloor hydrothermal circulation influences the thermal state and evolution of oceanic plates; alteration of the lithosphere and crustal pore waters; maintenance of extensive subseafloor microbial ecosystems; and diagenetic, seismic, and magmatic activity along plate-boundary faults [e.g., *Cowen et al.*, 2003; *Mottl and Holland*, 1978; *Peacock and Hyndman*, 1999; *Ranero et*

al., 2003; *Stein and Stein*, 1992]. Early seafloor heat flow measurements provided evidence of hydothermal circulation near mid-ocean spreading centers, helping to explain extreme variability of heat flow in areas where very high values were predicted by conceptual models of lithospheric creation [e.g., *Bullard and Day*, 1961; *Von Herzen*, 1959, 1963]. Areas that had low heat flow were interpreted to be places where cold ocean water recharged the permeable oceanic crust (or where underlying convection cells carried heat downward), whereas areas that had high heat flow were thought to be close to sites of hydrothermal discharge (or were located where convection cells upwelled) [e.g., *Lister*, 1972; *Williams et al.*, 1974].

[3] After a sufficient number of heat flow measurements had been acquired across the ocean basins, global data were compared to models of lithospheric cooling to evaluate the extent of hydrothermal circulation on ridge flanks, areas far from spreading centers [*Davis and Lister*, 1974; *Parsons and Sclater*, 1977; *Stein and Stein*, 1992; *Stein et al.*, 1995]. The physical basis for various lithospheric cooling models differ in important ways, but all standard models predict very similar heat flow trends for seafloor aged a few to ~100 Ma: heat flow decreases with $(\text{age})^{-1/2}$. It has become common practice in marine heat flow studies on ridge flanks to compare a suite of observations to standard lithospheric cooling curves to assess the possibility that heat is removed advectively from the crust. These comparisons are generally done with an average of many values collected in a single area, or with a composite (regional or global) mean of data available for a single crustal age, because local variability can result from conductive refraction, local convection, and other site-specific processes. As a rule, globally averaged heat flow values tend to follow trends predicted by conductive lithospheric cooling models when crustal ages are $\geq$65 Ma [*Parsons and Sclater*, 1977; *Stein and Stein*, 1992].

[4] Numerous studies have explored causes for the "end" of hydrothermal circulation within older seafloor, including sealing of cracks in the crust by mineral precipitation or mechanical compaction, thickening of the overlying sediment column, or reduction in heat input at the base of the plate [e.g., *Anderson and Hobart*, 1976]. In fact, variations in seafloor heat flow beyond what can be explained by conductive refraction, rapid sedimentation or slumping, changes in bottom water temperatures, or other local or regional processes may provide evidence of continuing hydrothermal circulation in basement even within seafloor far older than 65 Ma [e.g., *Embley et al.*, 1983; *Von Herzen*, 2004]. In addition, hydrothermal circulation may occur within basement rocks without generating any thermal signature at the seafloor if sediments are thick, basement relief is modest, and fluid flow rates are slow.

[5] *Noel* [1985] and *Noel and Hounslow* [1988] reported results of heat flow surveys over ~106 Ma seafloor of the Maderia Abyssal Plain (MAP) in the northeast Atlantic Ocean (Figure 1). The mean of 57 values reported in these papers is 60 ± 7 mW/m^2 (one standard deviation). This mean value is higher than predictions from standard lithospheric cooling models [e.g., *Davis and Lister*, 1974; *Parsons and Sclater*, 1977; *Stein and Stein*, 1994] and measurements from many other old seafloor sites [e.g., *Davis et al.*, 1984; *Detrick et al.*, 1986; *Larson et al.*, 1993; *Louden et al.*, 1987], which suggest that values of 50 ± 5 mW/m^2 might be expected for >100 Ma seafloor. In addition, local variations in heat flow measured in transects across essentially flat seafloor correlate positively with buried basement relief below thick sediments. This pattern is apparent in data from both studies, but measurements reported by *Noel* [1985] are more widely spaced (on the order of several kilometers), so the correlation between heat flow and basement relief is not as well expressed as that in the later study (for which typical measurement spacing is 300–500 m) [*Noel and Hounslow*, 1988].

[6] Two reasonable explanations for a positive correlation between seafloor heat flow and buried basement relief where the seafloor is flat are (1) conductive refraction resulting from higher thermal conductivity in basement having significant relief and (2) hydrothermal circulation in basement that (at least partly) homogenizes temperatures at the sediment-basement interface. As discussed in earlier studies and shown in the present paper, reasonable values of sediment and basement thermal conductivity result in seafloor heat flow variations as a result of conductive refraction that are significantly smaller than those observed along the MAP profiles. Hydrothermal circulation in basement is considered to be the most likely explanation for the measured pattern of seafloor heat flow in this area [*Noel*, 1985; *Noel and Hounslow*, 1988].

[7] *Noel and Hounslow* [1988] presented results from finite element models of conductive heat flow

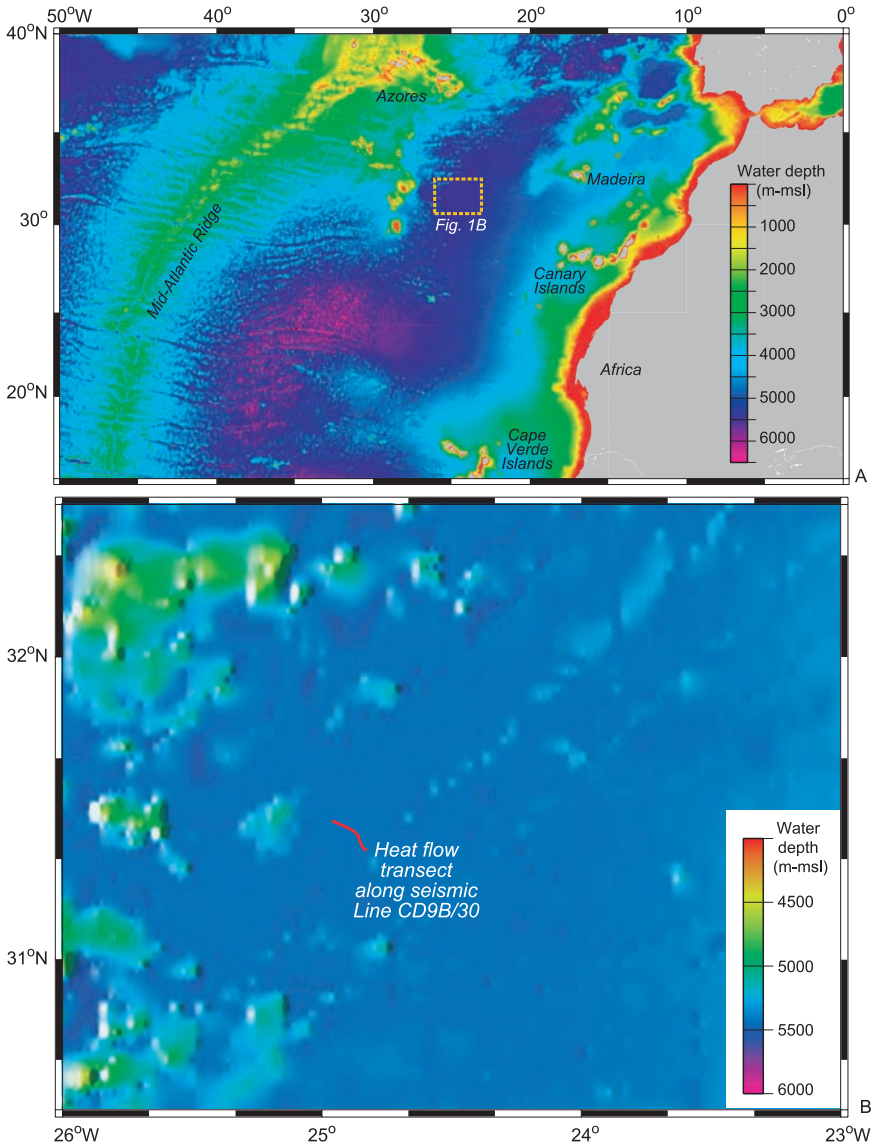

Figure 1. (a) Bathymetric map of north Atlantic Ocean showing regional setting (data from *Smith and Sandwell* [1997]). Dotted yellow box shows area of Figure 1b. (b) Bathymetric map of area around heat flow survey run along seismic line CD9B/30 (bathymetric data from *Smith and Sandwell* [1997]; heat flow positions from *Noel and Hounslow* [1988]). Note common basement outcrops to the west, north, and south of heat flow profile.

along several transects in order to evaluate the consistency of observations with this explanation, but to date there have been no coupled heat-fluid flow models of this region. Many modeling studies have explored hydrothermal processes in younger crust, but there has been only one modeling study of coupled fluid-heat flow in old (~100 Ma) seafloor, and those models were based on idealized (and largely arbitrary) patterns of basement relief and sediment thickness [*Fisher et al.*, 1994a]. In the present paper we show the first models of coupled heat-fluid flow through 106 Ma oceanic crust of the MAP, and use these models to elucidate the vigor and of fluid circulation in basement and the bulk hydrologic properties of old oceanic crust. We compare modeling results and interpretations to estimates of fluid circulation rates and crustal properties from other sites, and speculate on the nature of crustal evolution in old seafloor settings.

2. Heat Flow Data and Geologic Setting

[8] The MAP is centered ~30°N, 25°W on seafloor comprising the western edge of the African Plate, west of Madeira and the Canary Islands, south of the Azores, and north of the Cape Verde

Islands (Figure 1). The MAP is in the deepest part of the Canary Basin, where the water depth is ~5400 m. Much of the lithosphere in this area was generated at the slow-spreading Mid-Atlantic Ridge during the Cretaceous when there were few magnetic reversals, so the precise age of the crust is not known. Interpolation between magnetic anomalies 34 and M2 suggest that the study site is ~106 My old [*Noel*, 1985].

[9] Single-channel seismic data across the study area show that the seafloor is generally flat where sediment cover is complete, and there is often basement relief of 200–500 m at a typical wavelength of 2–5 km. Drilling in the area during ODP Leg 157 recovered sediments comprising clayey nannofossil mixed sediment and nannofossil clay turbidites interbedded with pelagic nannofossil ooze, mixed sediment, and clay [*Schmincke et al.*, 1995]. Turbidites are thicker and more common within shallower sediments, whereas deepest sediments tend to be more pelagic, with thin distal turbidite interbeds.

[10] Basaltic outcrops penetrate through sediments over part of the MAP, rising as much as 600–700 m above the surrounding seafloor (Figure 1b). Given characteristic sediment thicknesses of 400–500 m, these outcrops rise 1000–1200 m above the elevation of regional basement. Many of the basement outcrops are elongate or aligned to the northeast, subparallel to buried abyssal hill topography and the active spreading ridge to the west. MAP seismic and heat flow surveys were conducted where the seafloor is flat and sediment cover is essentially continuous [*Noel*, 1985; *Noel and Hounslow*, 1988], with the nearest basement outcrops located ~15–20 km west and 35–40 km to the north and south, based on swathmap and side scan data collected prior to ODP Leg 157 [*Schmincke et al.*, 1995; *Smith and Sandwell*, 1997]. There appear to be no basement outcrops located within 100–150 km to the east of the survey area.

[11] Heat flow through MAP sediments was determined in the early 1980s during a series of geological and geophysical studies intended to evaluate the suitability of the abyssal ocean floor for disposal of nuclear waste [e.g., *Francis*, 1984; *Searle et al.*, 1985]. Sites were sought having low-permeability sediments above more permeable basement rocks where there was little fluid flow. The MAP was targeted in part because it was expected that it would be inactive hydrothermally. This is an excellent area for the study of the causes of modest variations in heat flow below flat seafloor because of the consistent trends in basement relief and the extreme stability of seafloor thermal conditions [*Noel*, 1985].

[12] Two profiles of 21 heat flow measurements were made during R.R.S. Discovery cruise 144 [*Noel*, 1985]. Heat flow measurements were colocated along single-channel seismic profiles oriented perpendicular to major structural trends in basement, and were collected with a 4.2-m, violin-bow, multipenetration probe. This instrument included measurements of tilt and in-situ thermal conductivity. Two additional transects of 33 measurements were made using the same instrumentation during Charles Darwin cruise CD9B in an area adjacent to and south of the earlier survey [*Noel and Hounslow*, 1988]. Both surveys were navigated using transit satellites and by dead reckoning. Positions of individual heat flow measurements are known ±100 m relative to seismic profiles, but absolute locations have uncertainties of at least ±300 m.

[13] We focus the present modeling study on data collected during the second survey along profile CD9B/30 (Figures 1 and 2). This is an 18 km transect of heat flow measurements, separated by 200–500 m, along a seismic profile that shows ~500 m of basement relief buried below 170–570 m of sediment. Heat flow values along this profile range from 48 to 70 mW/m^2 (mean = 60 ± 6 mW/m^2). The highest heat flow values are located above buried basement highs and the lowest values are located above buried basement lows (Figure 2). None of the probe measurements made during the second survey generated a nonlinear thermal gradient or otherwise indicated nonconductive conditions within shallow sediments; in contrast several measurements made during the earlier survey were interpreted to indicate pore fluid advection from the seafloor at ~100 cm/yr. Considering the driving forces for hydrothermal circulation through ridge flanks and typical sediment permeabilities [e.g., *Fisher et al.*, 2003a; *Giambalvo et al.*, 2000; *Spinelli et al.*, 2004; *Wheat and Mottl*, 1994], it seems unlikely that pore waters move this rapidly though thick sediments on the MAP, but even if this were to occur, it would not result in significant advective heat extraction from the crust.

[14] *Noel and Hounslow* [1988] constructed and ran finite element models to evaluate whether contrasts in basement and sediment thermal conductivity and conductive refraction might explain the variability in seafloor heat flow seen along profile CD9B/30. A good match to observations

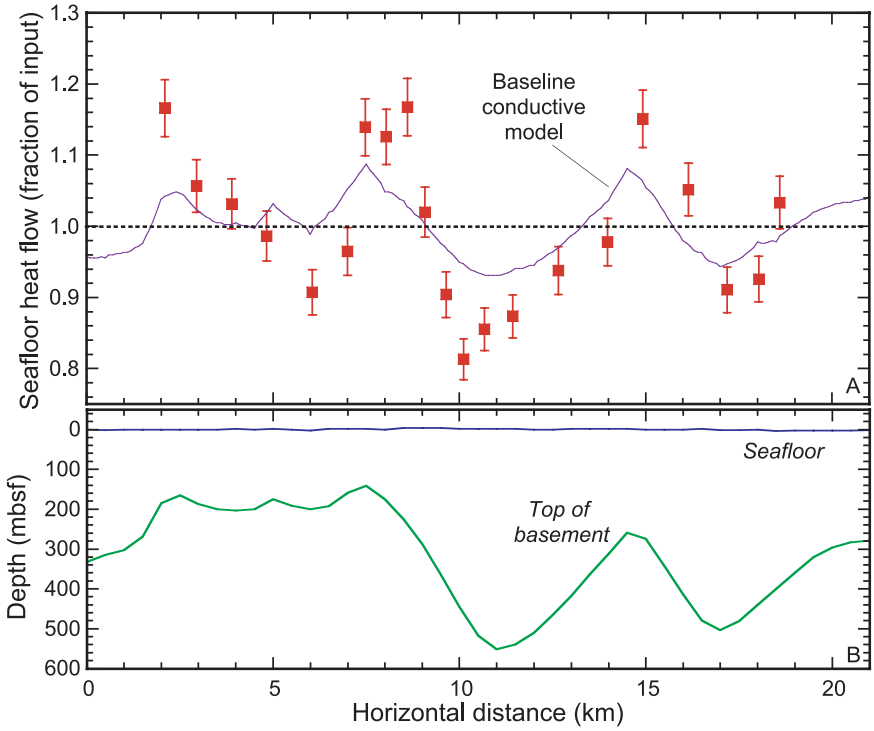

Figure 2. Interpreted heat flow and seismic data and conductive model results. Data from *Noel and Hounslow* [1988]. (a) Heat flow observations along seismic line CD9B/30 across 106 Ma seafloor of the Madeira Abyssal Plain, normalized to the mean of the transect (red squares). Vertical bars show deviations of ±5% from the reported values. Results of a two-dimensional conductive model calculation are shown for comparison (purple line). Horizontal dotted line shows normalized heat flow of 1, where seafloor output exactly matches input at the base of the model grid. Model formulation is discussed in the text and shown in later figures. Conductive model results are essentially identical to those shown by *Noel and Hounslow* [1988, Figure 5]. (b) Line-drawing interpretation of seismic line CD9B/30. Note positive correlation between local heat flow highs and lows (observed and modeled) and basement relief buried below thick sediments and a virtually flat seafloor. Observed variations in seafloor heat flow have greater amplitude than do conductive model results. The discrepancy between observations and conductive model results provides the primary motivation for additional modeling to evaluate crustal hydrogeology in this area.

could not be obtained with a reasonable conductive model. The observed pattern of heat flow highs and lows could be replicated using typical values for sediment and basement properties, but the amplitude of variability was 30–50% of that seen in the data. A thermal conductivity contrast between basement and sediment of ~3 was required to simulate the observed amplitude of seafloor heat flow, a contrast much larger that that typically found on oceanic ridge flanks.

3. Methods

[15] We prepared a suite of heat-fluid flow simulations, including conductive and advective processes, using FEHM [*Zyvoloski et al.*, 1996]. FEHM is a finite element model designed for simulating multiphase fluid, heat and solute transport on land. The code was modified for representation of ridge flank hydrothermal systems through use of a look-up table for single-phase fluid properties (density, enthalpy, viscosity) under an appropriate range of pressures and temperatures [*Harvey et al.*, 1997], and to allow for transient formation compressibility under nonisothermal conditions. The use of a fluid property formulation for pure water (rather than seawater) as a single phase is justified for the present study because pressure-temperature conditions are well above the critical point for either fresh water or seawater, property differences within the natural system are small, and it is differences in fluid density and compressibility, rather than absolute values, that govern the vigor and geometry of convection.

[16] Grids were created using seismic data to define the primary layers, with software for semi-automated mesh design [*Gable et al.*, 1996]. Sediment and rock properties were assigned on the

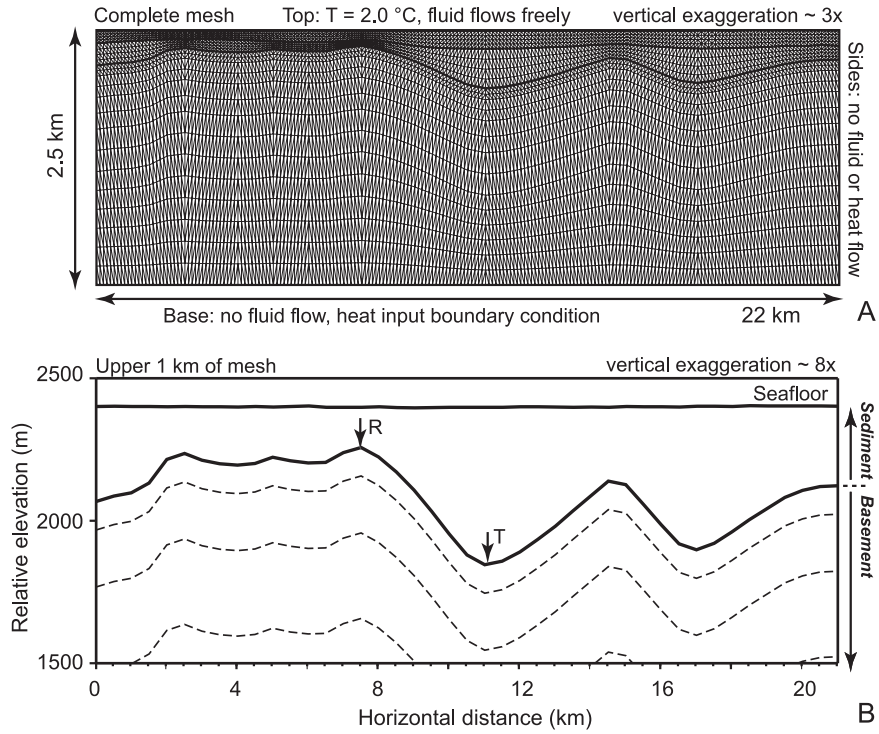

Figure 3. Numerical model configuration. (a) Complete finite element mesh and boundary conditions. Dark line marks sediment basement interface. Note vertical exaggeration (~3). (b) Layering of materials within the upper 1 km of the mesh. Dark lines mark seafloor and sediment-basement interface. Lighter, dashed lines mark boundaries between basement layers. Porosity was changed and basement layers were made more or less conductive and/or permeable to assess likely extent of hydrothermal circulation in basement. Note vertical exaggeration (~8). The contrast in upper basement temperatures at locations above a buried basement ridge (R) and trough (T) marked with arrows is discussed in the text.

basis of regional and global drilling results. FEHM is a transient model, but simulations were run until fluid and heat flow patterns reached a steady state in the case of stable convection, or a quasi-steady state in the case of oscillatory convection. The latter simulations were run until the heat flow pattern at the seafloor had stabilized, even if convection in underlying basement remained unstable.

[17] Seismic line CD9B/30 [*Noel and Hounslow*, 1988] was used to define the geometry of primary crustal layers (Figures 2 and 3). We assumed a two-dimensional representation for the upper oceanic crust, as is common for ridge-flank modeling [e.g., *Davis et al.*, 1997; *Fehn et al.*, 1983; *Fisher et al.*, 1990], but acknowledge that the actual fluid flow geometry may be three-dimensional. There are relatively few seismic lines with colocated heat flow data on the Maderia Abyssal Plain, but available seismic and bathymetric data suggest that the strongest gradients in basement relief are found along profiles perpendicular to the spreading ridge, cutting across abyssal hill topography. The interpretation that the dominant fluid flow geometry in this area is two-dimensional allows results of the present simulations to be compared to others from other, mainly younger, ridge flank settings.

[18] The modeling mesh is 22 km wide and 2.5 km tall (Figure 3). The base of the mesh has boundary conditions of constant heat flow and no fluid flow. No heat or fluid was allowed to pass across the vertical sides of the mesh, and the upper boundary was open to both heat and fluid flow and held at constant temperature (2°C) and hydrostatic pressure appropriate for the water depth. Horizontal node spacing was 100 m across the mesh, and vertical node spacing was variable, finer near the seafloor (particularly within the sediments above buried basement highs) and coarser within the deepest part of the grid (Figure 3).

[19] Heat input at the base of the mesh in all simulations was 49 mW/m^2, a value consistent with standard lithospheric cooling models. The mean observed heat flow in this area is ~10 mW/m^2 higher, but it is not clear whether this value

results from higher than expected heat input at the base of the plate, or is influenced by regional heating (during off-axis volcanic activity after the crust was formed) or by hydrothermal circulation. We normalized measured and calculated seafloor heat flow values for comparison between models and observations. A difference in heat input at the base of the mesh of 10 mW/m^2 will have no influence on normalized seafloor heat flow patterns; we tested several fully coupled simulations and found no significant difference in convection patterns in the crust associated with using the lower heat flow value.

[20] The sediment layer varied in thickness from ~150 to ~550 m, and bulk sediment properties were calculated as a function of depth below seafloor. Although sediments recovered in this area during drilling were lithologically variable at a fine scale, physical properties measurements made on core samples and geophysical data collected with wire line logs [*Schmincke et al.*, 1995] suggest that the porosity-depth (n versus z) trend is reasonably represented with an exponential relation of the form

$$n = 50 + 25\, e^{-(z/100)}, \quad (1)$$

where n is porosity (percent) and z is depth below seafloor (m).

[21] Bulk sediment thermal conductivity, λ_b, was calculated using a geometric mean mixing model ($\lambda_b = \lambda_f^n \lambda_g^{(1-n)}$), with fluid conductivity, λ_f, of 0.60 W/m-K and sediment grain conductivity, λ_g, of 1.6 W/m-K (the latter value being based on a fit of porosity and thermal conductivity data from core samples). This results in calculated bulk thermal conductivity values in sediments of $\lambda_b \sim 0.8$–1.0 W/m-K. Thermal conductivity measurements in this area during ODP Leg 157 yielded two groups of values, with fine-grained samples being similar to those used for modeling, and coarser layers giving values 10–30% [*Schmincke et al.*, 1995]. Within a highly layered system such as this, vertical conductive heat transport will be dominated by the layers with the lowest thermal conductivity, as represented in the models. As indicated by geochemical data recovered during drilling and in modeling results shown later, vertical heat transport through thick MAP sediments is dominantly conductive.

[22] Sediment permeability (k_s) was calculated from void ratio ($e = \frac{n}{1-n}$) using a relation derived for fine-grained marine sediments, $k_s = 10^{-18} e^5$ m^2 [*Bryant et al.*, 1974]. This permeability relation for fine-grained sediments is appropriate because, as with thermal conductivity and heat flow, layers with the lowest permeability will limit fluid flow. Sediment compressibility was calculated on the basis of laboratory measurements of consolidation and rebound properties [*Fisher et al.*, 1994b; *Giambalvo et al.*, 2000].

[23] Basement was divided into five primary layers with upper boundaries parallel to the sediment-basement interface. Bulk properties were held constant within each layer, but were varied between simulations. The shallowest four layers were 100, 200, 300, and 400 m thick, and the deepest layer had variable thickness so as to allow the base of the mesh to be flat (Figure 3). Porosity was assigned within the basement layers (top-down) to be 15%, 10%, 5%, 2% and 1%, based on wire line logging from numerous ocean crustal boreholes [e.g., *Bartetzko et al.*, 2001; *Jarrard and Broglia*, 1991; *Moos*, 1990; *Pezard and Anderson*, 1989]. As described later, we experimented with alternative basement porosity distributions (and associated thermal properties) and found these to have little influence on model results.

[24] Basement bulk thermal conductivity was assigned using a geometric mean mixing model and basement grain conductivity $\lambda_g = 2.05$ W/m-K. This grain conductivity is based on a suite of samples from old oceanic crust in the western Pacific Ocean [*Busch et al.*, 1992]. The resulting bulk thermal conductivity of basement was ~1.7–2.0 W/m-K, consistent with other measurements and estimates for the upper crust [e.g., *Becker et al.*, 1985; *Langseth et al.*, 1983; *Larson et al.*, 1993]. As discussed later, bulk thermal conductivity values were increased in some simulations as a proxy for efficient local convection.

[25] Basement permeability was held at 10^{-17} m^2 within the deepest crustal layer, but values were varied from 10^{-17} to 10^{-10} m^2 within the shallowest four layers to evaluate the consistency of resulting fluid and heat flow patterns on seafloor heat flow. This range of permeability values is based on upper crustal borehole measurements with a drill string packer or temperature log, results of earlier numerical studies, and the response of the upper oceanic crust to tidal and seismic perturbations [e.g., *Becker and Davis*, 2004; *Davis and Becker*, 2004; *Fisher*, 1998; *Spinelli and Fisher*, 2004]. Some earlier numerical studies included thin layers of extremely high permeability within the crustal

aquifer [*Fisher et al.*, 1994a; *Spinelli and Fisher*, 2004], but in this study we limited analyses to permeable layers no thinner than 100 m. This idealized representation is justified by the lack of measurements in old ocean crust, and by results of the simulations themselves, which suggest that permeability in upper MAP basement rocks need not be nearly as high as that measured or inferred within much younger crust.

4. Model Results

4.1. Baseline Conductive Simulations

[26] An initial set of baseline simulations was run to evaluate the possibility that variability in seafloor heat flow on the MAP along seismic line CD9B/30 could be explained by conductive refraction, to compare results to earlier conductive models, and to test the influence of a range of basement porosity and thermal conductivity structures on these results. Results are presented in a series of plots that compare modeled and measured seafloor heat flow, normalized to that input at the base of the mesh.

[27] The initial conductive simulation replicates earlier results [*Noel and Hounslow*, 1988] in which conductive refraction can account for heat flow variability of ±4–8%, whereas observed variability is ±10–20% (Figure 4). The variability in these new models (and in the original models) differs by 5–10% from that shown in another recent modeling study of conductive heat flow in this area [*Von Herzen*, 2004], but that study was based on calculations using a code that did not allow for fully two-dimensional heat transport away from sloping boundaries such as buried basement highs.

[28] We also ran conductive simulations that included constant basement porosity within the upper 1000 m of 2% and 15%, and associated thermal conductivity values calculated with a geometric mean mixing model (Figure 4a). Local differences in seafloor heat flow resulting from these simulations are ±1% relative to the standard conductive simulation in which basement porosity decreased from 15% to 2% within the upper 1000 m. We elected to use the decreasing basement porosity (and associated increasing thermal conductivity) model, herein referred to as the "baseline conductive" model in all subsequent discussion.

4.2. High Nusselt Number Proxy for Convective Mixing

[29] In earlier studies of ridge flank hydrothermal convection in young crust, the local influence of convective mixing was simulated conductively using a high Nusselt number (*Nu*) proxy [*Davis et al.*, 1997; *Spinelli and Fisher*, 2004; *Wang et al.*, 1997]. In these simulations the bulk thermal conductivity within layers in which convection was thought to occur was increased. This approach does not explicitly model advective heat transport, but it can yield insights as to the local efficiency of fluid circulation in thermally homogenizing adjacent regions in the crust, and is useful for qualitative evaluation of the relative vigor of convection. In a system in which there is net fluid flow through the system, as well as local mixing, the high *Nu* proxy may make advective heat extraction less efficient, because the proxy allows rapid conductive heat flow in a direction opposite to that of net advective transport [e.g., *Davis et al.*, 1999; *Rosenberget al.*, 2000; *Stein and Fisher*, 2003]. We did not simulate net through-flow of hydrothermal fluids in the present study, only local convection.

[30] We ran three sets of simulations using the high *Nu* proxy for convection in upper basement and examined what values of *Nu* provide the best match to observations of seafloor heat flow. The match between modeled and observed heat flow is not perfect even in the "best-fitting" of these high *Nu* simulations (nor in the fully coupled simulations shown later), and we made no attempt to adjust the geometry of the basement aquifer, sediment and basement thermal properties, or other parameters to achieve a better match. Discrepancies between modeled and observed seafloor heat flow may result from misinterpretation of seismic data, basement or fluid flow geometries that violate the two-dimensional approximation, highly heterogeneous permeability, or the geometry of the primary crustal aquifer not following the sediment-basement interface. We consider that a model provided an acceptable fit to observations if the seafloor heat flow highs and lows occur in roughly the right locations, above basement ridges and troughs, respectively, and if the magnitude of relative heat flow variations about the transect mean is appropriate.

[31] *Nu* values of 10, 5, and 2 in the uppermost 100 m, 300 m and 600 m of basement, respectively, were found to replicate both the 10–20% variability in seafloor heat flow and to place the heat flow highs and lows above local basement ridges and

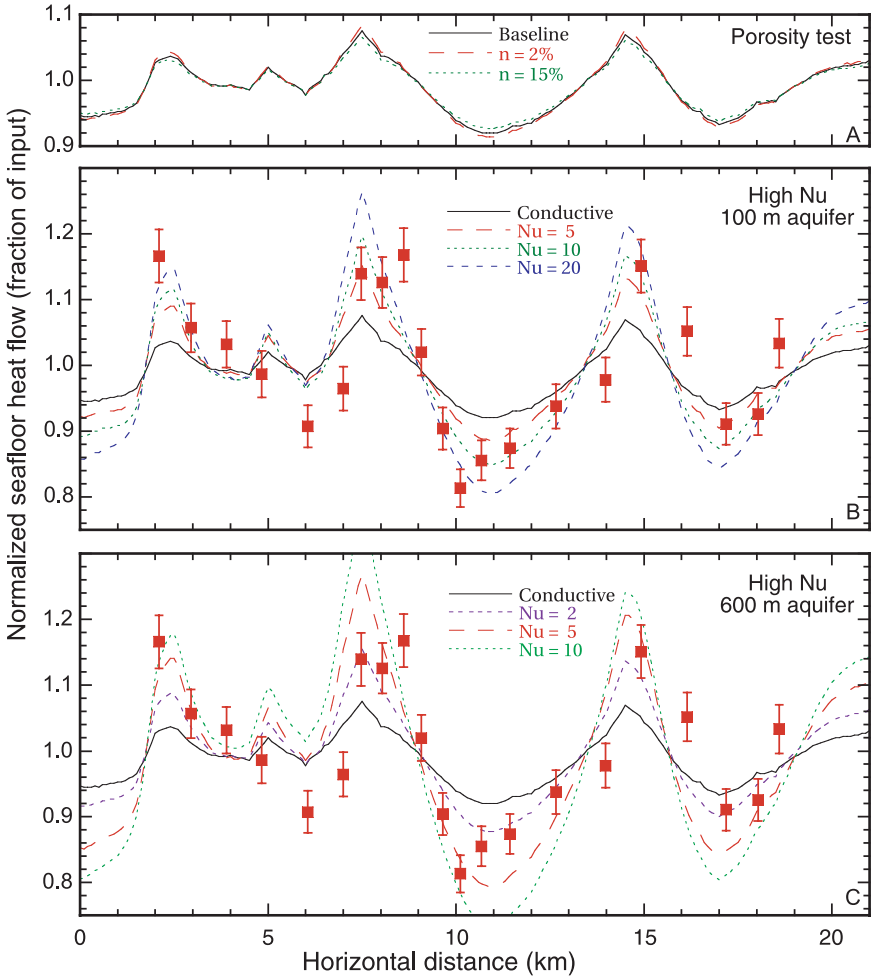

Figure 4. Normalized seafloor heat flow from conductive models and comparison with observations. (a) Comparison of conductive results using three porosity models. Baseline simulation has porosity decreasing from 15% to 2% within the upper 1 km of basement. Two additional (end-member) cases are shown, one with 2% porosity and one with 15% porosity in the upper 1 km of basement. Seafloor heat flow in these end-member cases differed from that in the baseline case by no more than 1%. The baseline case was used in all subsequent simulations. (b) Conductive simulation in which local convection within an aquifer in the upper 100 m of basement was simulated using a high *Nu* proxy. Values of *Nu* = 10-20 are most consistent with the field data. Symbols showing field data are as in Figure 2a. (c) Conductive simulation in which local convection within an aquifer in the upper 600 m of basement was simulated using a high *Nu* proxy. Values of *Nu* = 2–5 are most consistent with the field data. Symbols showing field data are as in Figure 2a.

troughs, respectively (Figure 4). These *Nu* values are considerably lower than *Nu* = 50–2000 inferred within 3.4–3.6 Ma oceanic crust on the eastern flank of the Juan de Fuca Ridge (JFR) [*Davis et al.*, 1997; *Spinelli and Fisher*, 2004], but in this younger setting there is almost complete isothermality of temperatures at the sediment-basement interface (±2–5°C), resulting in seafloor heat flow that varies by ±50% about the mean. In contrast, observations and these numerical studies of MAP crust suggest that only partial homogenization of the sediment-basement interface has been achieved, resulting in much smaller seafloor heat flow variations. The relation between *Nu* and the extent of basement isothermality where there is considerable basement relief is highly nonlinear. An initial boost in *Nu* reduces the temperature different between basement highs and lows by a few degrees, but increasingly greater *Nu* values are needed to achieve additional, equivalent reductions in the temperature difference between buried ridges and troughs.

[32] Under purely conductive conditions, the difference in uppermost basement temperatures between an adjacent buried ridge and trough along

the MAP heat flow transect (Figure 3b) is 18.3°C. A temperature difference of 15.0–15.3°C is suggested by the best-fitting conductive MAP simulations using the high *Nu* proxy. Variations in sediment thickness and basement elevation in the present study and those in the JFR flank studies on 3.4–3.6 Ma crust [*Davis et al.*, 1997; *Spinelli and Fisher*, 2004] are similar, and sediment and basement thermal properties are likely to be similar as well. Thus the contrast in thermal conditions at the sediment-basement interface between these two areas most likely results from a difference in the efficiency of heat transport resulting from fluid convection in basement. This may occur because the crustal aquifer in the MAP area is thinner, convection is slower, and/or bulk aquifer permeability is lower. These possibilities are considered in the fully coupled simulations described in the next section.

4.3. Fully Coupled Simulations

[33] Fully coupled simulations of fluid-heat flow used grids having the same geometry as those in the high *Nu* simulations. The conductive baseline simulation was used to generate thermal initial conditions, and these values were used to calculate initial pressure conditions. Ambient hydrostatic pressures were calculated by bootstrapping downward from the seafloor in 5 m increments, using trilinear interpolation to estimate temperatures at each step. We also ran a subset of simulations beginning with a cold hydrostatic initial condition rather than ambient hydrostatic.

[34] Unlike earlier studies in which the initial pressure condition was important in determining the final geometry of convection in the oceanic crust [*Spinelli and Fisher*, 2004; *Stein and Fisher*, 2003], we found no measurable influence of initial conditions on final fluid and heat flow patterns or rates. This is because the MAP simulations include fluid convection that is essentially sealed within basement below thick sediments, and because basement permeabilities and heat input below the crustal aquifer are relatively low, both of which lead to fluid flow rates that are significantly slower than those within younger crust. Initial conditions can predetermine the geometry and pattern of coupled, transient models of fluid circulation in the oceanic crust when there is sufficiently rapid circulation and enough of a temperature difference between areas of upflow and downflow (for example, in areas of discharge and recharge through exposed basement outcrops), so as to allow formation of a hydrothermal siphon [*Fisher et al.*, 2003a; *Spinelli and Fisher*, 2004; *Stein and Fisher*, 2003]. This did not occur in the fully coupled MAP simulations.

[35] Coupled simulations in which the greatest basement permeability was confined to only the uppermost 100 m below the sediment-basement interface failed to replicate observed seafloor heat flow patterns, even when basement aquifer permeability was extremely high (Figure 5a). Convection cells in basement were too small in these simulations to move heat efficiently across horizontal distances of 3–5 km, up and down the sides of buried basement ridges. When the basement aquifer was extended to include the upper 300 m of crust, higher permeability (10^{-11} to 10^{-10} m^2) led to the formation of wider convection cells, leading to variations in seafloor heat flow similar in magnitude to those observed (Figures 5b and 6). These wider cells move heat efficiently up the sides of the buried basement ridges; in fact, lateral heat advection was so efficient in the case of $k_b = 10^{-10}$ m^2 that the magnitude of heat flow highs and lows exceeded those observed (Figure 5). Smaller convection cells also formed along areas where upper basement was relatively flat, leading to short wavelength (500–1000 m) variations in seafloor heat flow of ±2–5% (Figures 5b and 6c).

[36] This effect was enhanced when uppermost 600 m of basement was made permeable. Basement permeability $k_b = 10^{-12}$ to 10^{-11} m^2 generated the appropriate magnitude of heat flow variations (±10–20%), but local oscillations in areas of flat basement were as large as those associated with larger-scale basement relief (Figure 5c). Seafloor measurements in this area are too widely spaced to be certain that the observed heat flow pattern is not aliased, but one might expect to encounter greater variability in field data if small convection cells such as these formed in oceanic crust of the MAP. Additional simulations were run in which the basement aquifer was 300–600 m thick and permeability was anisotropic, being 100 times greater in the horizontal direction, but resulting convection and heat flow patterns were little different from those in equivalent isotropic simulations.

[37] Rates of fluid circulation in basement in basement required to achieve the observed level of seafloor heat flow variation are on the order of 10^{-8} to 10^{-7} m/s, 0.3–3 m/yr (Figure 6). Slower rates of fluid flow in upper basement do not move heat rapidly enough between basement ridges and troughs to reduce the difference in basement tem-

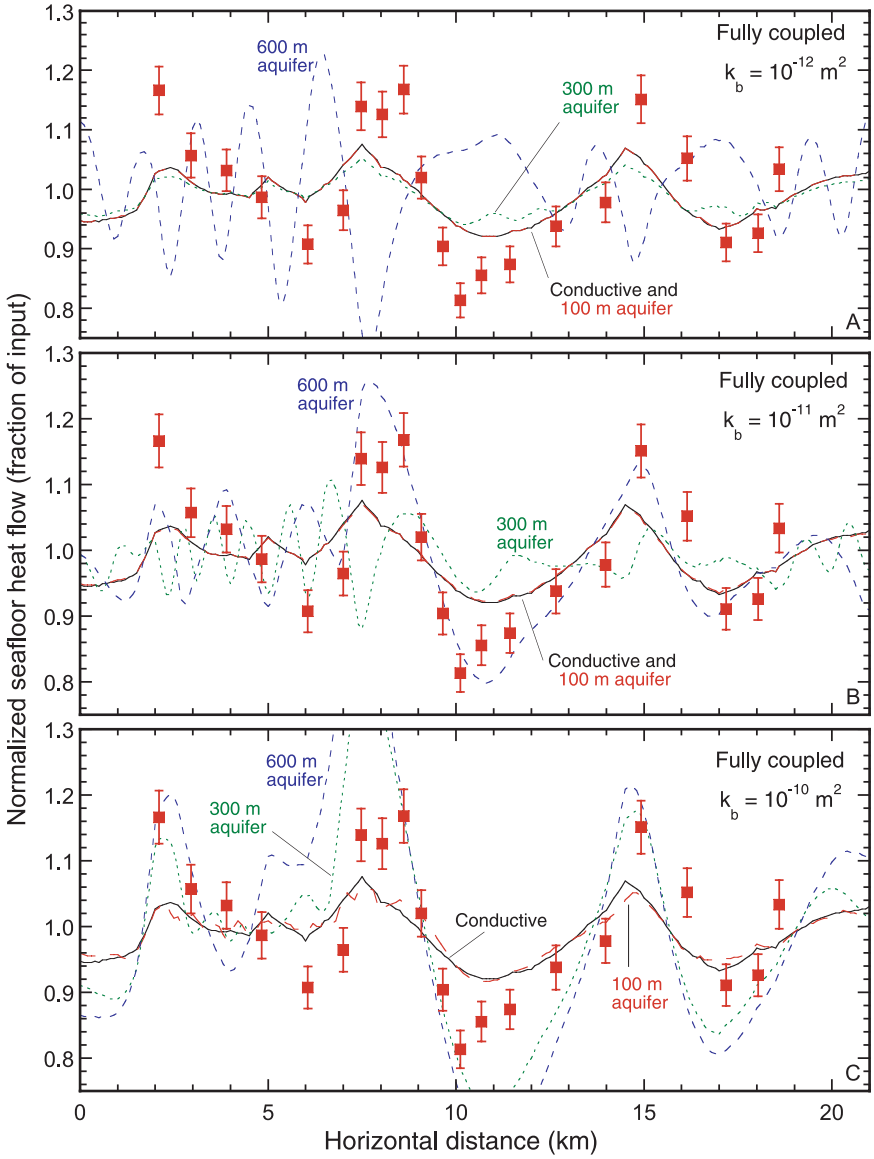

Figure 5. Normalized seafloor heat flow from fully coupled models and comparison with observations. In each plot, solid black line shows seafloor heat flow from conductive baseline model. Symbols showing field data are as in Figure 2a. (a) 100 m permeable aquifer in uppermost basement. Colored dashed and dotted lines show results for basement aquifer permeabilities of 10^{-12} m^2 to 10^{-10} m^2, as indicated in legend. Simulations with basement aquifer having permeability of 10^{-13} m^2 resulted in seafloor heat flow essentially identical to that from the conductive baseline simulation. (b) 300 m permeable aquifer in uppermost basement. Lines showing seafloor heat flow for fully coupled simulations are as in Figure 5a. (c) 600 m permeable aquifer in uppermost basement. Lines showing seafloor heat flow for fully coupled simulations are as in Figure 5a.

peratures and redistribute seafloor heat flow as observed.

5. Discussion: Comparison to Other Sites and Global Implications

[38] Seafloor thermal data suggest that the bulk basement permeability of the upper 300–600 m of MAP crust may be on the order of 10^{-10} to 10^{-12} m^2. This range of values is broadly consistent with the global data set of single-hole packer and thermal flowmeter measurements in upper oceanic crust [*Fisher*, 2005], but most of these data were collected in much younger seafloor. The range of 10^{-10} to 10^{-12} m^2 is somewhat higher than that determined in ODP Hole 801C, a 157–165 Ma site in the western Pacific Ocean [*Larson et al.*, 1993], where bulk permeability was $\sim 10^{-13}$ m^2. Hole 801C is the only hole in which

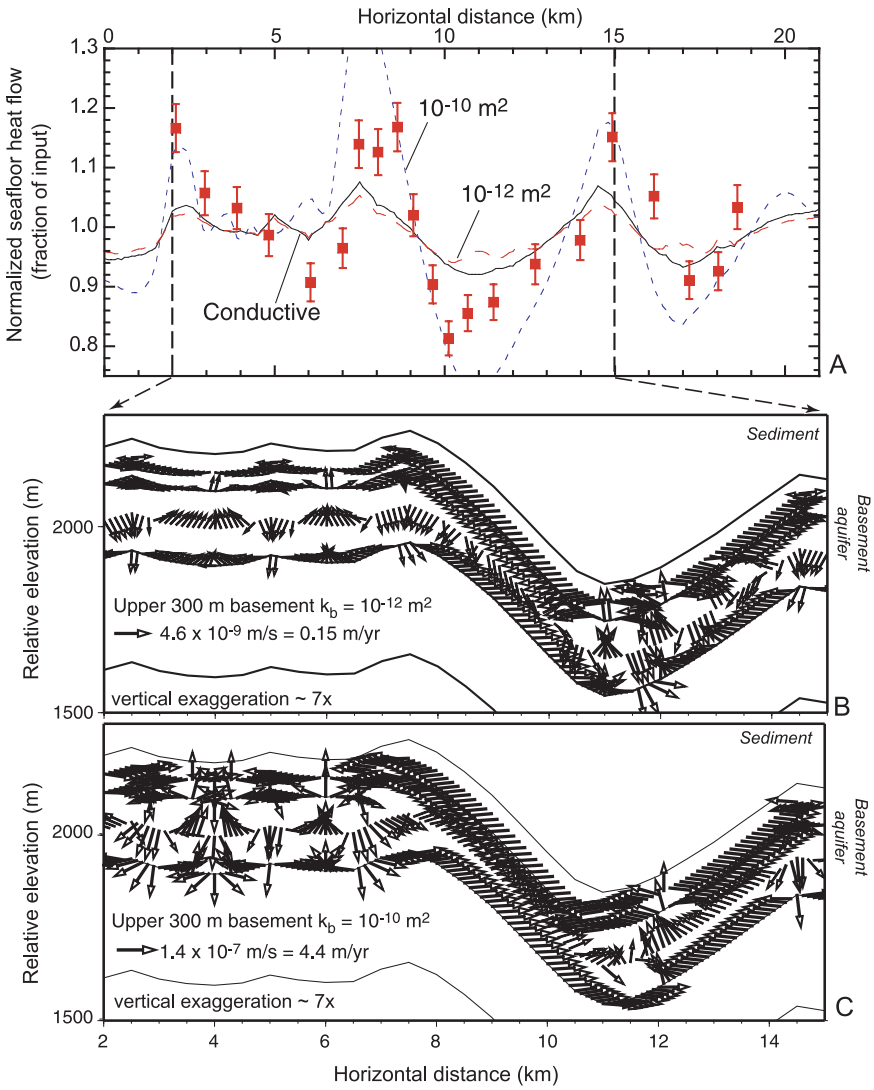

Figure 6. Seafloor heat flow and fluid vectors in simulations with permeable aquifer in upper 300 m of basement. (a) Normalized seafloor heat flow. Dashed and dotted lines indicate results of fully coupled model predictions for basement aquifer permeability $k_b = 10^{-12}$ m^2 and $k_b = 10^{-10}$ m^2, as labeled. Solid line is result for conductive reference simulation. Symbols showing field data are as in Figure 2a. (b) Fluid flow vectors for aquifer permeability $k_b = 10^{-12}$ m^2. (c) Fluid flow vectors for aquifer permeability $k_b = 10^{-10}$ m^2. Vectors are log normalized onto to a linear scale; reference vector length shown for each plot is the largest vector. Vectors smaller than $\sim 5 \times 10^{-5}$ times the magnitude of the reference vector are not shown. With basement permeability of 10^{-12} m^2 (Figure 6b), weak convection cells develop within flat basement areas (horizontal distance 2–8 km), and some steeply dipping areas develop a single convection cell (horizontal distance 8–10 km). Fluid convection is sluggish in this simulation, so little heat is redistributed advectively within the basement aquifer. This simulation underestimates the extent of local thermal advection in basement, as indicated by small variations in seafloor heat flow. With basement permeability of 10^{-10} m^2 (Figure 6c), small convection cells are well developed in flat basement areas, and single cells form on the sides of buried basement ridges. As a result, variations in seafloor heat flow are large and vary smoothly. This simulation overestimates the extent of local thermal advection in basement, as indicated by variations in seafloor heat flow.

packer measurements have been made in basaltic oceanic crust that is older than 8 Ma. The crust around Hole 801C may not be typical of old seafloor, since the most permeable zone is associated with an intensely altered region between tholeiitic and alkalic basalts, emplaced at the spreading center and off axis (~8 m.y. later), respectively.

[39] Single-hole packer experiments test the region immediately around a borehole, whereas larger-

scale analyses, including coupled fluid-heat modeling studies, often suggest bulk permeabilities that are significantly greater [*Becker and Davis*, 2003; *Becker and Fisher*, 2000; *Fisher*, 1998]. Thus the finding that bulk permeabilities suggested by modeling of MAP crust are greater than those indicated by packer and flowmeter testing in crustal holes elsewhere is not surprising.

[40] Although high *Nu* (conductive) simulations were successful in replicating observed seafloor heat flow patterns when the basement aquifer was only 100 m thick (Figure 4a), fully coupled simulations with a thin aquifer were not able to produce a similar result (Figure 5a). This is because the higher permeabilities implied by the higher *Nu* values resulted in formation of very small convection cells within the thin aquifer, and this geometry was inefficient at moving significant heat laterally in upper basement. A more structured permeability distribution, in which thin channels help to focus lateral fluid flow might provide the necessary efficiency, as seen in numerical studies of younger crust [*Fisher et al.*, 1994a; *Spinelli et al.*, 2004]. These earlier studies also showed that within a basement aquifer, most of the flow can be focused through a small number of thin channels, resulting in extremely efficient lateral heat transport. As noted earlier, we have not completed additional fully coupled models of MAP crust with permeable layers thinner than 100 m because of a lack of observational constraints, but core and geophysical logging data from old seafloor suggest that, as at younger sites, the upper oceanic crust is highly layered and heterogeneous on a scale of meters to tens of meters [e.g., *Bartetzko et al.*, 2001; *Broglia and Moos*, 1988; *Jarrard et al.*, 1995; *Larson et al.*, 1993].

[41] Additional insight is provided through comparison of permeabilities estimated for upper MAP crust on the basis of coupled models and extrapolation of permeability trends predicted from an analysis of global heat flow data [*Fisher and Becker*, 2000]. Consideration of heat flow anomalies, driving forces and typical path lengths for extraction of measurable heat during ridge-flank hydrothermal circulation allowed calculation of bulk permeability-age trends of the upper oceanic crust (Figure 7). For sedimentation rates on the order of 5 m/my and a hydrothermal aquifer in the upper 300–600 m of oceanic crust, effective permeabilities on the order of 10^{-11} to 10^{-10} m^2 are suggested for ~65 Ma seafloor. This analysis cannot be extended beyond 65 Ma because it is based on the mean global heat flow anomaly, which approaches zero at ~65 Ma. The bulk permeability of 106 Ma MAP basement suggested by numerical models overlaps the lower end of the range suggested for 65 Ma seafloor on the basis of global heat flow data. This suggests that the reduction of basement permeability apparent in relatively young ridge flanks may slow considerably within older seafloor. Perhaps this results, in part, from the relative hydrologic isolation of the crustal aquifer from the overlying ocean in old crust, which may help to maintain elevated crustal temperatures and slow the deposition of hydrothermal precipitates that could clog the largest (most important) fluid pathways.

[42] An analysis of available data from 58 old seafloor sites suggests that many have remained hydrothermally active, even after the mean heat flow in these locations becomes consistent with lithospheric predictions (Figure 8) [*Von Herzen*, 2004]. The fraction of older sites that remain hydrothermally active appears to decrease with increasing age, but the lack of an observable seafloor thermal anomaly does not preclude the occurrence of hydrothermal circulation at depth. Fluid flow may occur below thick sediments at rates that are not detectable with seafloor sediment probes [e.g., *Fisher et al.*, 1994a]. In addition, it is difficult to evaluate the possibility of continuing hydrothermal circulation at many old sites because they lack colocated and well-navigated heat flow and seismic data [*Von Herzen*, 2004].

[43] The MAP may differ in one important way from many similarly aged sites around the world: mean heat flow in this area is ~20% greater on average than predicted by standard models for lithospheric cooling. One explanation for this observation is that the thermal age of the plate has been "reset" by off-axis volcanism, perhaps associated with the large outcrops ~5° west of the survey area (Figure 1a). Another possibility is that the elevated seafloor heat flow in this area results from large-scale lateral advection in basement, but this would require that there be one or more nearby areas where seafloor heat flow is commensurately low. There could be trends of higher and lower heat flow associated with recharge and discharge through basement outcrops west, north, and south of the MAP (Figure 1b), but there are insufficient data at present to evaluate this possibility. There may be additional outcrops even closer to the survey area that are hydrogeologically important but are too small to be revealed by available

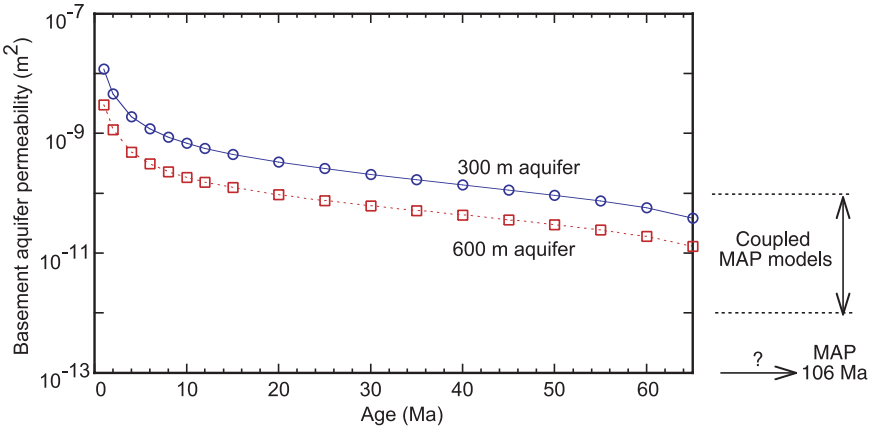

Figure 7. Comparison of effective basement permeability estimated in this study and the permeability versus age trend for 1–65 Ma seafloor predicted by an analysis of global heat flow and sedimentation patterns, and characteristic driving forces available to drive ridge-flank convection (analysis modified from *Fisher and Becker* [2000]). The permeability versus age trend for 1–65 Ma seafloor was calculated for a mean sedimentation rate of 5 m/m.y., broadly appropriate for the MAP, which helps to determine the depth of the basement aquifer and thus the forces available to drive ridge flank circulation. Two curves were calculated for aquifer thicknesses of 300 and 600 m. The global calculations suggest that bulk permeability in the basement aquifer must be on the order of 10^{-11} m^2 to 10^{-10} m^2 by the time the ocean crust reaches 65 Ma, whereas the numerical models shown earlier suggest that upper MAP basement has a bulk permeability of 10^{-12} m^2 to 10^{-11} m^2. Thus it appears that the loss of basement permeability suggested by the global heat flow data set during 1–65 Ma may continue after measurable advective heat loss from the crust ends.

(mainly satellite-based) bathymetric data [*Smith and Sandwell*, 1997]. Recent studies of younger flank sites suggest that basement fluids may travel rapidly across tens of kilometers within oceanic crust between outcrops [*Fisher et al.*, 2003a, 2003b]. It is not clear if this kind of large-scale transport can occur within old oceanic crust, or if such flows could efficiently redistribute lithospheric heat at the scale implied by the extent of the MAP anomaly.

6. Conclusions

[44] Heat flow data colocated with seismic data from the Madeira Abyssal Plain in the north Atlantic Ocean show local variability of 10–20% that correlates with basement relief buried below thick sediments. Earlier models showed that conductive refraction associated with the contrast in the thermal conductivity of basement and sediments cannot explain these variations. Conductive simulations in which local mixing in upper basement is represented with a high *Nu* proxy suggest that *Nu* ~2–10 is required to account for observed heat flow variations, assuming that convection is restricted to the upper 100–600 m of basement. These *Nu* values are much lower than those estimated at younger ridge flank sites, but nevertheless are sufficient reduce the temperature difference between upper basement on buried ridges and troughs by ~20%.

[45] Fully coupled simulations suggest that an aquifer in upper basement that is just 100 m thick may be inconsistent with observations. When permeability is raised sufficiently so as to allow rapid fluid flow in basement, small convection cells develop that are inefficient at moving heat laterally. However, the formation of small cells can be inhibited by forcing fluid flow to occur within thin channels in the crust [*Fisher et al.*, 1994a; *Spinelli and Fisher*, 2004]. When the basement aquifer in upper basement is made 300–600 m thick and permeability is sufficiently high, 10^{-12} to 10^{-10} m^2, broad convection cells develop and heat is transferred rapidly up the sides of buried basement ridges, redistributing seafloor heat flow to roughly match observations. These simulations also include formation of small-scale convection cells where basement is relatively flat, leading to high-frequency variations in seafloor heat flow that may not be present in field observations. Other permeability structures may be consistent with field data, including those in which fluid flow is channelized within thin layers, faults, or other conduits in the upper crust, but there are insufficient observations in this area to justify more detailed modeling of upper crustal permeability at present.

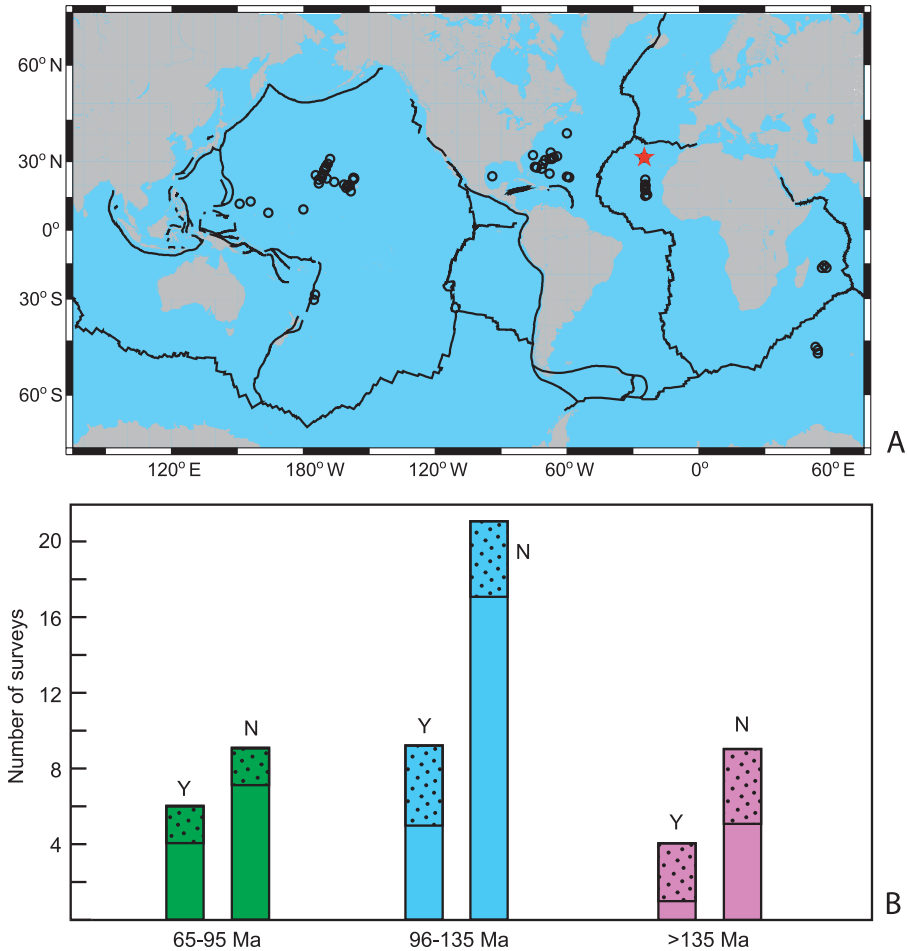

Figure 8. Compilation of heat flow studies on old seafloor sites (modified from *Von Herzen* [2004]). (a) Map showing distribution of old sites where there are seafloor heat flow profiles that allow assessment of potential for hydrothermal circulation. Location of MAP survey sites is shown with red star. (b) Histogram showing the frequency of positive and negative indications for continuing hydrothermal circulation in seafloor older than 65 Ma, based on seafloor heat flow measurements. Data are divided into three bins, as shown. Y, data suggest that there is hydrothermal circulation; N, data suggest that there is not hydrothermal circulation. Parts of bars filled with dots indicate results that are ambiguous, either because there is insufficient seismic coverage to evaluate the influence of conductive refraction resulting from basement relief or because observed heat flow variations are only marginally significant.

[46] The estimated bulk permeability for MAP seafloor, 10^{-12} to 10^{-10} m^2 in the upper 300–600 m of basement, is consistent with a permeability evolution model for the oceanic crust in which permeability decreases rapidly within young seafloor, and decreases more slowly at older sites [e.g., *Fisher and Becker*, 2000]. The MAP is part of a group of older crust sites where there is compelling thermal evidence for continuing hydrothermal circulation in basement, long after the typical 65 Ma age at which the oceanic crust stops losing heat advectively [*Von Herzen*, 2004]. The MAP may be unusual in that the mean heat flow determined from two surveys is higher than predicted by standard lithospheric cooling models, perhaps because of reheating during off-axis volcanic activity, or because of large-scale redistribution of heat by basement fluids.

Acknowledgments

[47] Funding in support of this work was provided by the U.S. National Science Foundation (OCE-0001892), the U.S. Science Support Program for IODP (T301A7), and the Institute for Geophysics and Planetary Physics/Los Alamos National Laboratory (1317).

References

Anderson, R. N., and M. A. Hobart (1976), The relationship between heat flow, sediment thickness, and age in the eastern Pacific, *J. Geophys. Res.*, *81*, 2968–2989.

Bartetzko, A., P. Pezard, D. Goldberg, Y.-F. Sun, and K. Becker (2001), Volcanic stratigraphy of DSDP/ODP Hole 395A: An interpretation using well-logging data, *Mar. Geophys. Res.*, *22*, 111–127.

Becker, K., and E. Davis (2003), New evidence for age variation and scale effects of permeabilities of young oceanic crust from borehole thermal and pressure measurements, *Earth. Planet. Sci. Lett.*, *201*(3–4), 499–508.

Becker, K., and E. Davis (2004), In situ determinations of the permeability of the igneous oceanic crust, in *Hydrogeology of the Oceanic Lithosphere*, edited by E. E. Davis and H. Elderfield, pp. 189–224, Cambridge Univ. Press, New York.

Becker, K., and A. Fisher (2000), Permeability of upper oceanic basement on the eastern flank of the Endeavor Ridge determined with drill-string packer experiments, *J. Geophys. Res.*, *105*(B1), 897–912.

Becker, K., M. Langseth, R. Anderson, and M. Hobart (1985), Deep crustal geothermal measurements, Hole 504B, Costa Rica Rift, Legs 69, 70, 83, and 92, *Initial Rep. Deep Sea Drill. Proj.*, *83*, 405–418.

Broglia, C., and D. Moos (1988), In-situ structure and properties of 110-Ma crust from geophysical logs in DSDP Hole 418A, *Proc. Ocean Drill. Program Sci. Results*, *102*, 29–47.

Bryant, W. R., A. P. Deflanche, and P. H. Trabant (1974), Consolidation of marine clays and carbonates, in *Deep-Sea Sediments: Physical and Mechanical Properties*, edited by A. L. Inderbitzen, pp. 209–244, Springer, New York.

Bullard, E. C., and A. Day (1961), The heat flow through the floor of the Atlantic, *Geophys. J. R. Astron. Soc.*, *4*, 282–292.

Busch, W. H., P. R. Castillo, P. A. Floyd, and G. Cameron (1992), Effects of alteration on physical properties of basalts from the Pigafetta and East Mariana basins, *Proc. Ocean Drill. Program Sci. Results*, *129*, 485–500.

Cowen, J. P., S. J. Giovannoni, F. Kenig, H. P. Johnson, D. Butterfield, M. S. Rappé, M. Hutnak, and P. Lam (2003), Fluids from ageing ocean crust that support microbial life, *Science*, *299*, 120–123.

Davis, E. E., and K. Becker (2004), Observations of temperature and pressure: Constraints on ocean crustal hydrologic state, properties, and flow, in *Hydrogeology of the Oceanic Lithosphere*, edited by E. E. Davis and H. Elderfield, pp. 225–271, Cambridge Univ. Press, New York.

Davis, E. E., and C. R. B. Lister (1974), Fundamentals of ridge crest topography, *Earth Planet. Sci. Lett.*, *21*, 405–413.

Davis, E. E., C. R. B. Lister, and J. C. Sclater (1984), Toward determining the thermal state of old ocean lithosphere: Heat flow measurements from the Blaka-Bahama Outer Ridge, *Geophys. J. R. Astron. Soc.*, *78*, 507–545.

Davis, E. E., K. Wang, J. He, D. S. Chapman, H. Villinger, and A. Rosenberger (1997), An unequivocal case for high Nusselt-number hydrothermal convection in sediment-buried igneous oceanic crust, *Earth Planet. Sci. Lett.*, *146*, 137–150.

Davis, E. E., D. S. Chapman, K. Wang, H. Villinger, A. T. Fisher, S. W. Robinson, J. Grigel, D. Pribnow, J. Stein, and K. Becker (1999), Regional heat-flow variations across the sedimented Juan de Fuca Ridge eastern flank: Constraints on lithospheric cooling and lateral hydrothermal heat transport, *J. Geophys. Res.*, *104*(B8), 17,675–17,688.

Detrick, R. S., R. P. V. Herzen, B. Parsons, D. Sandwell, and M. Dougherty (1986), Heat flow observations on the Bermuda Rise and thermal models of mid-plate swells, *J. Geophys. Res.*, *91*, 3701–3723.

Embley, R., M. Hobart, R. Anderson, and D. Abbott (1983), Anomalous heat flow in the northwest Atlantic: A case for continued hydrothermal circulation in 80 MY crust, *J. Geophys. Res.*, *88*, 1067–1074.

Fehn, U., K. Green, R. P. Von Herzen, and L. Cathles (1983), Numerical models for the hydrothermal field at the Galapagos Spreading Center, *J. Geophys. Res.*, *88*, 1033–1048.

Fisher, A. T. (1998), Permeability within basaltic oceanic crust, *Rev. Geophys.*, *36*(2), 143–182.

Fisher, A. T. (2005), Marine hydrogeology: Future prospects for major advances, *Hydrogeol. J.*, doi:10.1007/s10040-004-0400-y.

Fisher, A. T., and K. Becker (2000), Channelized fluid flow in oceanic crust reconciles heat-flow and permeability data, *Nature*, *403*, 71–74.

Fisher, A. T., K. Becker, T. N. Narasimhan, M. G. Langseth, and M. J. Mottl (1990), Passive, off-axis convection on the southern flank of the Costa Rica Rift, *J. Geophys. Res.*, *95*, 9343–9370.

Fisher, A. T., K. Becker, and T. N. Narasimhan (1994a), Off-axis hydrothermal circulation: Parametric tests of a refined model of processes at Deep Sea Drilling Project/Ocean Drilling Program site 504, *J. Geophys. Res.*, *99*, 3097–3121.

Fisher, A. T., K. Fischer, D. Lavoie, M. Langseth, and J. Xu (1994b), Hydrogeological and geotechnical properties of shallow sediments at Middle Valley, northern Juan de Fuca Ridge, *Proc. Ocean Drill. Program Sci. Results*, *139*, 627–647.

Fisher, A. T., et al. (2003a), Hydrothermal recharge and discharge across 50 km guided by seamounts on a young ridge flank, *Nature*, *421*, 618–621.

Fisher, A. T., C. A. Stein, R. N. Harris, K. Wang, E. A. Silver, M. Pfender, M. Hutnak, A. Cherkaoui, R. Bodzin, and H. Villinger (2003b), Abrupt thermal transition reveals hydrothermal boundary and role of seamounts within the Cocos Plate, *Geophys. Res. Lett.*, *30*(11), 1550, doi:10.1029/2002GL016766.

Francis, T. J. G. (1984), A review of I. O. S. research into the feasibility of high-level radioactive waste disposal in the oceans, *Sci. Total Environ.*, *35*, 301–323.

Gable, C. W., H. E. Trease, and T. A. Cherry (1996), Geological applications of automatic grid generation tools for finite elements applied to porous flow modeling, in *Numerical Grid Generation in Computational Fluid Dynamics and Related Fields*, edited by B. K. Soni et al., pp. 1–9, Miss. State Univ. Press, Mississippi State.

Giambalvo, E. R., A. T. Fisher, J. T. Martin, L. Darty, and R. P. Lowell (2000), Origin of elevated sediment permeability in a hydrothermal seepage zone, eastern flank of the Juan de Fuca Ridge, and implications for transport of fluid and heat, *J. Geophys. Res.*, *105*, 913–928.

Harvey, A. H., A. P. Peskin, and S. A. Kline (1997), NIST/ASME steam properties, 49 pp., Natl. Inst. for Stand. and Technol., Gaithersburg, Md.

Jarrard, R. D., and C. Broglia (1991), Geophysical properties of oceanic crust at Sites 768 and 770, *Proc. Ocean Drill. Program Sci. Results*, *124*, 75–90.

Jarrard, R. D., R. L. Larson, A. T. Fisher, and L. J. Abrams (1995), Geophysical aging of oceanic crust: Evidence from Hole 801C, *Proc. Ocean Drill. Program Sci. Results*, *144*, 649–662.

Langseth, M. G., J. Cann, J. Natland, and M. Hobart (1983), Geothermal phenomena at the Costa Rica Rift: Background to objectives for drilling at Deep Sea Drilling Project sites 501, 504, 505, *Initial Rep. Deep Sea Drill. Proj*, *69*, 5–29.

Larson, R. L., A. T. Fisher, R. Jarrard, and K. Becker (1993), Highly permeable and layered Jurassic oceanic crust in the western Pacific, *Earth Planet. Sci. Lett.*, *119*, 71–83.

Lister, C. R. B. (1972), On the thermal balance of a mid-ocean ridge, *Geophys. J. R. Astron. Soc.*, *26*, 515–535.

Louden, K. E., D. O. Wallace, and R. C. Courtney (1987), Heat flow and depth versus age for the Mesozoic Northwest Atlantic Ocean: Results from the Sohm abyssal plain and implications for the Bermuda Rise, *Earth Planet. Sci. Lett.*, *83*, 109–122.

Moos, D. (1990), Petrophysical results from logging in DSDP Hole 395A, ODP Leg 109, *Proc. Ocean Drill. Program Sci. Results*, *106/109*, 237–253.

Mottl, M. J., and H. D. Holland (1978), Chemical exchange during hydrothermal alteration of basalt by seawater I. Experimental results for major and minor components of seawater, *Geochim. Cosmochim. Acta*, *42*, 1103–1115.

Noel, M. (1985), Heat flow, sediment faulting and porewater advection in the Madeira abyssal plain, *Earth Planet. Sci. Lett.*, *73*, 398–406.

Noel, M., and M. W. Hounslow (1988), Heat flow evidence for hydrothermal convection in Cretaceous crust of the Madiera Abyssal Plain, *Earth Planet. Sci. Lett.*, *90*, 77–86.

Parsons, B., and J. G. Sclater (1977), An analysis of the variation of ocean floor bathymetry and heat flow with age, *J. Geophys. Res.*, *82*, 803–829.

Peacock, S. M., and R. D. Hyndman (1999), Hydrous minerals in the mantle wedge and the maximum depth of subduction thrust earthquakes, *Geophys. Res. Lett.*, *26*, 2517–2520.

Pezard, P., and R. N. Anderson (1989), Morphology and alteration of the upper oceanic crust from in-situ electrical experiments in DSDP/ODP Hole 504B, *Proc. Ocean Drill. Program Sci. Results*, *111*, 133–146.

Ranero, C. R., J. Phipps Morgan, and R. von Huene (2003), Bending-related faulting and mantle serpentinization at the Middle America Trench, *Nature*, *405*, 367–373.

Rosenberg, N., A. Fisher, and J. Stein (2000), Large-scale lateral heat and fluid transport in the seafloor: Revisiting the well-mixed aquifer model, *Earth Planet. Sci. Lett.*, *182*, 93–101.

Schmincke, H.-U., P. P. E. Weaver, and J. Firth (Eds.) (1995), *Proceedings of the Ocean Drilling Program, Initial Reports*, vol. 157, 843 pp., Ocean Drill. Program, College Station, Tex.

Searle, R. C., P. Schultheiss, P. P. E. Weaver, M. J. Noel, R. B. Kidd, C. L. Jacobs, and Q. L. Huggett (1985), Great Meteor East (Distal Maderia Abyssal Plain): Geological studies of its suitability for disposal of heat-emitting radioactive wastes, Inst. of Oceanogr. Sci., Southampton, UK.

Smith, W. H. F., and D. T. Sandwell (1997), Global sea floor topography from satellite altimetry and ship depth soundings, *Science*, *277*, 1956–1962.

Spinelli, G. A., and A. T. Fisher (2004), Hydrothermal circulation within rough basement on the Juan de Fuca Ridge flank, *Geochem. Geophys. Geosyst.*, *5*(2), Q02001, doi:10.1029/2003GC000616.

Spinelli, G. A., L. Zühlsdorff, A. T. Fisher, C. G. Wheat, M. Mottl, V. Spieß, and E. R. Giambalvo (2004), Hydrothermal seepage patterns above a buried basement ridge, eastern flank of the Juan de Fuca Ridge, *J. Geophys. Res.*, 109, B01102, doi:10.1029/2003JB002476.

Stein, C. A., and S. Stein (1992), A model for the global variation in oceanic depth and heat flow with lithospheric age, *Nature*, *359*, 123–137.

Stein, C., and S. Stein (1994), Constraints on hydrothermal heat flux through the oceanic lithosphere from global heat flow, *J. Geophys. Res.*, *99*, 3081–3095.

Stein, C. A., S. Stein, and A. M. Pelayo (1995), Heat flow and hydrothermal circulation, in *Seafloor Hydrothermal Systems: Physical, Chemical, Biological and Geological Interactions*, *Geophys. Monogr. Ser.*, vol. 91, edited by S. E. Humphris et al., pp. 425–445, AGU, Washington, D. C.

Stein, J. S., and A. T. Fisher (2003), Observations and models of lateral hydrothermal circulation on a young ridge flank: Numerical evaluation of thermal and chemical constraints, *Geochem. Geophys. Geosyst.*, *4*(3), 1026, doi:10.1029/2002GC000415.

Von Herzen, R. (1959), Heat-flow values from the southeastern Pacific, *Nature*, *183*, 882–883.

Von Herzen, R. P. (1963), Geothermal heat flow in the Gulfs of California and Aden, *Science*, *140*, 1207–1208.

Von Herzen, R. P. (2004), Geothermal evidence for continuing hydrothermal circulation in older (>60 Ma) ocean crust, in *Hydrogeology of the Oceanic Lithosphere*, edited by E. E. Davis and H. Elderfield, pp. 414–450, Cambridge Univ. Press, New York.

Wang, K., J. He, and E. E. Davis (1997), Influence of basement topography on hydrothermal circulation in sediment-buried oceanic crust, *Earth. Planet. Sci. Lett.*, *146*, 151–164.

Wheat, C. G., and M. J. Mottl (1994), Hydrothermal circulation, Juan de Fuca Ridge eastern flank: Factors controlling basement water composition, *J. Geophys. Res.*, *99*, 3067–3080.

Williams, D. L., R. P. Von Herzen, J. G. Sclater, and R. N. Anderson (1974), The Galapagos Spreading Centre, lithospheric cooling and hydrothermal circulation, *Geophys. J. R. Astron. Soc.*, *38*, 587–608.

Zyvoloski, G. A., B. A. Robinson, Z. D. Dash, and L. L. Trease (1996), Users manual for the FEHMN application, Los Alamos Natl. Lab., Los Alamos, N. M.